

See discussions, stats, and author profiles for this publication at: <https://www.researchgate.net/publication/314521050>

Label-free impedance biosensors for Point-of-Care diagnostics

Chapter · March 2017

DOI: 10.5599/obp.11.6

CITATIONS

9

READS

2,921

2 authors, including:



Cheng-Hsin Chuang

National Sun Yat-sen University

116 PUBLICATIONS 828 CITATIONS

SEE PROFILE

Some of the authors of this publication are also working on these related projects:



Tactile sensor [View project](#)



Mechanical property of Materials [View project](#)

Chapter

8

**LABEL FREE IMPEDANCE BIOSENSORS FOR
POINT OF CARE DIAGNOSTICS**

Cheng-Hsin Chuang* and Muhammad Omar Shaikh

Department of Mechanical Engineering
Southern Taiwan University of Science and Technology, Tainan 71005,
Taiwan

*Corresponding author: chchuang@stust.edu.tw

Contents

8.1. INTRODUCTION.....	173
8.2. WHY IMPEDANCE BIOSENSORS FOR POINT OF CARE DIAGNOSTICS?	173
8.3. GROWING NEED FOR FEASIBLE AFFINITY BIOSENSORS	174
8.4. BASIC OF IMPEDANCE BIOSENSING	177
8.5. ELECTRODES.....	179
8.6. IMPEDANCE MEASUREMENTS.....	182
8.7. DATA ANALYSIS USING EQUIVALENT CIRCUIT MODELS.....	184
8.8. IMMOBILIZATION STRATEGIES.....	187
8.9. MODEL OF AN IMPEDANCE IMMUNOSENSOR.....	189
8.10. RECENT DEVELOPMENTS IN IMPEDANCE IMMUNOSENSORS	194
8.10.1. Non-Faradaic impedance immunosensors	195
8.10.2. Faradaic impedance immunosensors	196
8.10.3. Amplification strategies	197
8.11. CONCLUSION	198
REFERENCES	199

8.1. INTRODUCTION

This chapter introduces the basic concepts and fundamentals of impedance and its use as a label free transduction scheme for biosensing applications. An increasing trend towards the development of impedance biosensors is currently being observed due to the viability of this method for the direct detection of affinity biorecognition events and suitability for point of care applications. Herein, antibody-antigen affinity interactions have been used as an example and the model of an immunosensor utilizing both Faradaic and non-Faradaic impedance detection has been presented. Finally, impedimetric immunosensors are reviewed and novel designs and amplification strategies are discussed.

8.2. WHY IMPEDANCE BIOSENSORS FOR POINT OF CARE DIAGNOSTICS?

Although clinical analysis has traditionally been performed in well-equipped laboratories by trained professionals, this approach is not feasible in the absence of these optimal conditions, as is often the case in underdeveloped areas and low resource settings. In such situations, biosensors which are analytical devices that enable detection of specific analytes may be the only way to obtain trustworthy diagnosis. In general, there has been a global effort to make healthcare more patient oriented so that tests can be performed at the “point of care” which can be anywhere from the home to out in the field. This would reduce the number of visits to the doctor or a centralized laboratory and would enable effective real time diagnosis. Hence it is no surprise that current research is oriented towards developing biosensors that are viable for point of care testing [1,2]. Most biosensors are “affinity-based” since they utilize a bioreceptor which has a strong affinity to the target and can selectively capture it as in the case of antibody-antigen interactions and DNA-DNA hybridization. Currently, the most common way for signal transduction utilized in affinity biosensors is optical as is the case with the well-established Enzyme-Linked Immunosorbent Assay (ELISA). Another example of optical affinity biosensors is paper based Lateral Flow Assays (LFA) like pregnancy strips that utilize gold nanoparticles for achieving calorimetric detection. While extremely suitable for point of care testing where a yes/no answer is required, they are less suitable for quantitative analysis and can suffer from false positives, especially when complex colored samples are used. Optical transduction normally requires the use of labels (gold nanoparticles, fluorescent tags, quantum dots or signal amplification using enzymes) to achieve sensitive and selective detection of analyte. However, there are issues associated with labeling which

include additional costs, inherent multistep nature of analyses and potentially perturbative and non-specific signals. This has led to an increased interest in techniques that require no labeling and are inherently more facile and suitable for point of care diagnostics. Among them, electrical/electrochemical transduction based biosensors have attracted widespread interest for label free analysis with reduced complexity during signal acquisition. They possess an innate sensitivity and simplicity which makes them arguably the most practical and quantifiable diagnostic technique for detection of biomolecules [3,4]. In very general terms, an affinity biosensor utilizing electrochemical transduction reports the capturing of a biological target by a bioreceptor modified electrode interface through a generated current or voltage signal (or perturbation thereof) [5]. Based on the interrogation technique used, electrical biosensors can be broadly categorized as potentiometric, amperometric/voltammetric and impedimetric. In particular, impedance based electrical transduction, where the applied electrical signal is alternating as opposed to direct, can be used to analyze both the resistive and the capacitive changes at the electrode surface over a wide frequency range during affinity binding. This analytical approach, known as electrochemical impedance spectroscopy (EIS), is an effective strategy for the non-destructive probing of complex bio-recognition events [6,7] and has been utilized in a wide range of biosensors ranging from bacteria and pathogen detection to immunosensing and DNA characterization [8-11]. When a target analyte is captured by the receptor functionalized electrode surface, it alters the electrical properties (*e.g.* capacitance, charge transfer resistance) of the electrode/solution interface which can be analyzed using EIS. Thus, EIS can be used for real time and direct monitoring of affinity binding events without the use of labeling compounds. Furthermore, EIS biosensors possess attractive characteristics often associated with electrical biosensors which include low cost, low power, scalability, ease of miniaturization and multiplexing capability which makes them promising candidates for use in point of care diagnostics.

8.3. GROWING NEED FOR FEASIBLE AFFINITY BIOSENSORS

A biosensor utilizes a bio sensing element which interacts with the analyte being tested and the biological response is converted by the transducer into a measurable signal. The biosensing element can be either proteins, enzymes, nucleic acids, antibodies, tissues, cells or receptors while the transducer may be optical, electrochemical, thermometric, piezoelectric, magnetic, or micromechanical. Thus biosensors can be categorized based on either the biosensing element or the transduction mechanism utilized and combine the selectivity of biological systems with the computing power of a microprocessors to obtain a quantifiable signal that correlates to the analyte

concentration. Based on the type of bio recognition event that they monitor, biosensors can be broadly classified as being either catalytic or affinity in nature [12].

Catalytic biosensors incorporate enzymes, whole cells or tissues as the biosensing element and detect the presence of analytes by producing electroactive signals. Usually, the target analyte is either oxidized or reduced in the presence of an enzyme. Owing to their complex molecular structure, enzymes can selectively detect very small concentrations of analyte even in complex mixtures like urine or blood [5]. Personal glucose monitoring devices, which are the most successful commercial biosensors, employ the enzyme glucose oxidase to detect glucose concentration in whole blood. While enzymes possess inherent selectivity and high biocatalytic activity, they are unable to detect several analytes of interest which cannot be catalyzed by a specific enzyme or are not commonly found in living systems. In such cases, affinity biosensors can be used which detect analytes in an alternative way.

Affinity biosensors, monitor the binding of a target to immobilized recognition elements on transducer surfaces. They take advantage of the selective binding properties of certain biomolecules, most often antibodies, receptors or nucleic acids. The molecular recognition in affinity biosensors is mostly determined by the complementary shape and size of the binding site to the analyte of interest [12]. Biomolecules with high affinity and specificity for the given target are desirable. Most often observed in this category are immunosensors that take advantage of versatile antibody libraries. If antibodies can be raised against something, then an immunosensor can be created for the target including bacteria, viruses, drugs and other chemicals and can thus have widespread applications [12,13]. Nucleic acids have also been used as recognition elements to detect complementary nucleic acids, or as aptamers, which are engineered oligonucleotide or peptide biomolecules selected for affinity against a specific target. Affinity biosensing can be either performed in a single step (binding of target analyte to produce a measurable signal) or more commonly by multistep protocol using signal amplification techniques (enzyme or nanoparticle labeling) to improve sensitivity. Here, we will be focusing on direct and label free affinity biosensing for analyte detection.

While catalytic biosensors have enjoyed widespread commercial success in the biosensors market, only a few label free affinity biosensors have been commercialized to date. Currently, the immobilization of affinity bioreceptors on solid surfaces while still retaining their stability and activity is one of the major challenges facing affinity biosensors in general. Furthermore, since detection of analytes is often performed in complex fluids, it is vital that the sensor surface must be highly selective towards the target analyte so that non-specific interactions due to presence of interferences can be minimized. Associated with the issue of selectivity is the limit of detection which is the smallest concentration of target analyte that can be detected. Although label free affinity biosensors can achieve low limits of detection in deionized water

or buffer spiked samples, this is more difficult to achieve in real biological samples which often contain large amounts of non-target interferences. Finally, issues with reproducibility (affected by factors like pH and ionic strength of sample), usability, durability and cost of instrumentation all affect the commercialization of label free affinity biosensors.

The most common and developed type of electrochemical transduction used for biosensors is the amperometric approach which monitors the current related to the oxidation and/or reduction of an electroactive species at the surface of a working electrode [14]. By coupling an amperometric sensor to an enzyme, as in a glucose biosensor, one gets the additional advantage of the high specificity and selectivity offered by the enzyme. The catalytic reaction occurring at the surface of a working electrode, when an enzyme is in the presence of its substrate, gives rise to a current proportional to the concentration of the species produced or consumed. In an enzyme based biosensor, a molecule needs to be transformed into another molecule by an enzyme to obtain an electroactive signal. EIS overcomes this problem and enables non-electroactive detection of molecules. While amperometry/voltammetry have commonly been used to detect electroactive signals produced during catalytic reactions, they are less suitable for direct detection of affinity events where they often require redox active labels to achieve sensitive and specific detection. For affinity biosensors, EIS has some important advantages over amperometry. The active site where the biologically mediated redox reaction is taking place should be in close proximity to the surface of the electrode. While redox mediators can be used to improve accessibility to the electrode, the detection is then limited by the mediator mass transfer. Furthermore, additional redox active species might be present in the sample solution that will interfere with the amperometric signal if the applied DC bias is not chosen correctly. Impedance based biosensing enables the direct detection of affinity binding events by monitoring interfacial changes occurring at the electrode surface. If the problems associated with non-specific binding can be overcome and electrode geometries and surface areas can be optimized (*e.g. via* nanotexturing or using nanoparticles), EIS can be a very useful transduction mechanism for sensitive and label free monitoring of biorecognition events.

8.4. BASIC OF IMPEDANCE BIOSENSING

Impedance based biosensors normally utilize the formation of a recognition complex between a bioreceptor (*e.g.* antibody) and its corresponding specific analyte (*e.g.* antigen) in a thin film configuration on the electrode surface [15]. This complex formation alters the interfacial capacitance and charge transfer resistance at the electrode/electrolyte interface. Impedance biosensors can sensitively monitor changes at the electrochemical interface and are powerful analytical devices when electrode surfaces are controllably modified with biomaterials. Impedance measurements are performed in alternating current (AC) steady state with a constant direct current (DC) bias and commonly involve the application of small amplitude perturbing sinusoidal voltage at a particular frequency and observing the corresponding current response. This process can be repeated over a range of frequencies, thus yielding an impedance spectrum. The resulting current sine wave varies in time and amplitude with respect to the applied voltage sine wave and the ratio $V(t)/I(t)$ is defined as the Impedance (Z) and can be mathematically expressed as:

$$Z(\omega) = \frac{1}{Y} = \frac{V_0 \sin(\omega t)}{I_0 \sin(\omega t + \theta)}$$

where V_0 and I_0 are the maximum voltage and current signals, ω is the excitation frequency in rad. s^{-1} ($\omega = 2\pi f$, f is frequency in Hz), t is time, θ is the phase shift between the voltage-time and current-time functions and Y is the complex conductance or admittance that is inversely proportional to the obtained impedance. Impedance is a complex value affected by multiple factors, which can be described either by the magnitude ($|Z|$) and the phase shift (θ) or alternatively as a combination of real (Z_{re}) and imaginary (Z_{im}) parts of the impedance. When the applied voltage and current waves are in phase ($\theta = 0$), the system behaves like a pure ohmic resistor. However, in reality electrochemical systems are complex and the impedance consists of an imaginary part that can be related to double layer charging due to charge separation at the electrode/electrolyte interface which is analogous to a capacitor. Furthermore, effects of mass transport and reaction kinetics also contribute to this imaginary component. Thus biosensors utilizing impedance transduction are often analyzed in terms of a combined effect of resistance and capacitance.

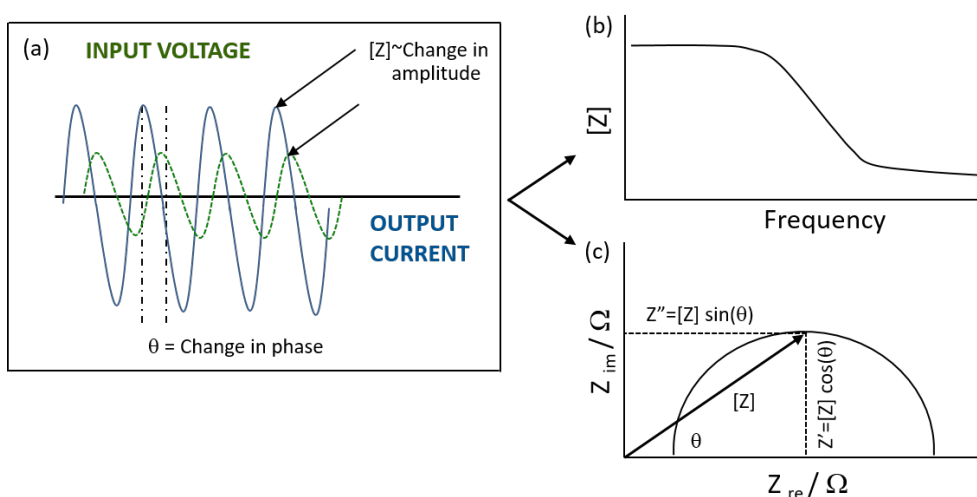


Figure 1. Electrochemical Impedance Spectroscopy (EIS) measurement and analysis: (a) Comparing the applied voltage (time) and the resultant current (time) functions to determine the phase shift (θ) and absolute impedance ($[Z]$) of the system. The resulting information can be presented in the form of (b) Bode plots, which can compare the absolute impedance or the phase shift versus frequency, or as (c) Nyquist plots, which compare the real (Z'_{re}) and imaginary (Z''_{im}) components of the resulting impedance.

It is important to consider the voltage magnitude (both the sinusoidal perturbation and the DC bias) when utilizing EIS for affinity binding. The amplitude of the AC voltage should be low (generally less than 50 mV) so as to obtain a linear current response and ensure non-destructive probing of the biomolecular layer [16]. High amplitude voltage results in increased force on charged biomolecules (*e.g.* proteins) which also applies to the DC bias conditions as both interfacial charge transfer and capacitance depend on the applied potential. If performed correctly, EIS has the capability to sensitively monitor interfacial changes without damaging or even disturbing the affinity binding event which is a big advantage over amperometric or voltammetric approaches where higher voltages are utilized. In addition, since the voltage is alternating as opposed to direct, electrolysis of the electrode is prevented and readout can be more accurate. The most popular formats for evaluating electrochemical impedance data are the Nyquist and Bode plots as shown in Figure 1 (b,c). In the Nyquist format, the imaginary impedance component (Z'') is plotted against the real impedance component (Z') at each excitation frequency giving information about the electrified interface and the electron transfer reaction whereas in the Bode format, both the logarithm of the absolute impedance, $[Z]$ and the phase shift, ϕ , are plotted against the logarithm of the excitation frequency.

Depending on whether there is a redox related charge transfer at the electrode/solution interface, EIS biosensors can be categorized as either being Faradaic or non-Faradaic. In electrochemistry, Faradaic approaches involve actual physical transfer of electrons or ions from the electrode to the solution and *vice versa*. However, in the absence of this charge transfer as can be the case in an insulated electrode surface, transient currents can still flow and this effect is analogous to the charging of capacitor. In reality, most electrode/solution interfaces in biosensors often have a combination of Faradaic and non-Faradaic components. EIS biosensors based on the Faradaic approach utilize an added redox probe at an appropriately biased electrode surface (near the oxidation potential so that none of the redox states are depleted). Affinity binding leads to a change in the electron exchange between the electrode and the redox probe. This resistance to charge transfer can be monitored in a quantifiable manner and will mostly increase after target recognition. In contrast, non-Faradaic or capacitive biosensors, do not require the addition of any redox probes and are inherently simpler and more amenable for point of care testing with the ability to make measurements (mostly related to the change in interfacial capacitance during affinity binding) at a single frequency. Nonetheless, this methodology will detect any species binding onto the interface, without discriminating between specific and unspecific capture. Because of this, it is of extreme importance that the electrode surface is conveniently functionalized so as to ensure that only the target is being bound and thus detected. The only way to guarantee this is to perform carefully chosen negative controls in parallel. Surprisingly, most publications in the field do not include such negative controls to confirm the specificity of the detected signals.

8.5. ELECTRODES

Like other electrochemical transduction mechanisms, EIS requires a minimum of two electrodes to measure the impedance of the electrode-solution interface. In a two electrode system, an electrical contact is made between the working electrode and the solution using a counter electrode and the bias potential at the working electrode is fixed with respect to the open circuit potential. It is therefore difficult to accurately identify the working electrode potential which is particularly important for Faradaic approaches where it must be maintained close to the oxidation potential of the redox species used. When inserted in a solution, the working electrode-solution interface has a built in potential that is affected by electrode microstructure, surface composition and ionic strength of the solution. Therefore, in order to have good control over the bias potential applied at the working electrode-solution interface, a three electrode configuration is often used with the addition of a reference electrode. The reference electrode, which maintains a fixed and reproducible built in potential between its metal contact and the electrolyte

allows a known voltage to be applied between the working electrode and the solution. Silver-silver chloride is the most common type of reference electrode used in impedimetric biosensors. In an ideal arrangement, the reference electrode should be placed as close as possible to the working electrode and along the current path between the working and counter electrodes. In order to eliminate the contribution of the counter electrode to the total observed impedance, it should be made of an inert material with an area much larger than the working electrode. Generally, the choice of material used for electrode fabrication in impedimetric biosensors is crucial as it effects assay sensitivity, cost and the ability to adopt different immobilization protocols (gold electrodes are often used because of the ease of forming self-assembled monolayers using thiol chemistry). Electrodes for impedimetric biosensors are often made of inert metals like gold and platinum and various forms of carbon which include graphene, epoxy graphite and glassy carbon among others. Irrespective of whether a two or three electrode system is utilized, it is crucial to choose a consistent and reproducible electrode design based on geometrical factors like size, separation and distribution [17].

While three electrode systems reduce background effects and enable sensitive and reliable measurements, interdigitated electrodes (IDEs) have often been used to fabricate impedance based affinity biosensors because of their inherent simplicity and amenability to miniaturization which makes them suitable for point of care applications. IDEs generally consist of two pairs of working electrodes that consist of parallel metal fingers that are interdigitated and separated by an insulating material [18,19]. IDEs possess several advantages like low ohmic drop, fast attainment of steady-state, increased signal-to-noise ratio, use of small solution volumes and rapid kinetics of reaction [20,21]. Owing to the geometry of IDEs, current flow mainly occurs very close to the surface and therefore shows much higher sensitivity for analyzing surface changes as compared to conventional electrodes. The biorecognition element can either be immobilized on top of the IDE electrodes or in the gap between the electrode fingers. Highly sensitive sensor response requires strong electrical fields that can be achieved by reducing the distance between the electrodes [22]. The typical distance between the electrode fingers used for biosensing is about 1–10 μm and is limited by the fabrication protocol. Theoretical analysis shows that about 80 % of the current between electrodes which are separated by a distance of 250 nm will flow in a layer no higher than 250 nm above the surface and will therefore significantly improve sensitivity of direct binding detection [23]. Although IDEs are very well suited for impedance measurements because of their well-defined geometry and the reproducibility of their fabrication techniques, they do have some problems. As the distance between electrodes becomes smaller, the chances of suffering short circuiting of the electrode set caused by the presence of the sample also increase, which may result in a ruined measurement. Another disadvantage of interdigitated electrodes lies in the difficulty of using them in a three-electrode

configuration, which can hardly be overcome by using an external reference electrode. In the latter case, artifacts appear due to the remoteness of the reference electrode from the current path between the working and auxiliary electrode structures. Electrodes for impedimetric detection, including IDEs, can also be manufactured using low cost and scalable technologies like screen printing on.

To successfully develop impedance biosensors for point of care testing, it is key that the electrode fabrication process is simple, cost effective and scalable for mass production. The use of printing techniques is an obvious step towards mass production of devices at a relatively low cost when compared to the use of semiconductor cleanroom techniques, which involve multiple processing steps using complex and expensive facilities. In particular, screen-printing technology has opened new exciting opportunities for detection of analytes outside a centralized laboratory due to their linear output, low power requirement, quick response and high sensitivity. Furthermore, the whole electrode system, including working, counter and reference electrodes can be printed on the same substrate surface. IDEs and a conventional three electrode setup have also been screen printed on polymer, paper and ceramic substrates, thus enabling disposable biosensor applications as shown in Figure 2.

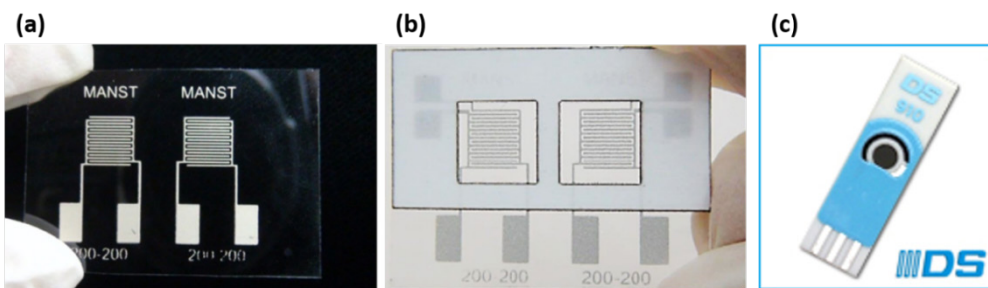


Figure 2. Electrodes fabricated by screen printing on disposable substrates. (a) IDEs on plastic. (b) IDEs on paper. (c) Three electrode setup on ceramic manufactured by DropSens (www.dropsens.com/).

8.6. IMPEDANCE MEASUREMENTS

A potentiostat is generally used for performing impedance measurements by imposing a desired voltage across the electrode-electrolyte interface and measuring the resulting current response. In electrical terminology, it consists of a feedback loop that controls the current flowing through the counter electrode so that the potential of the working electrode can be maintained at a constant level as compared to the reference electrode. The working electrode is held at ground and the current flowing through it can be analyzed *via* a transimpedance amplifier. If the counter and reference electrode are the same as in the case of IDEs, then no feedback loop is necessary but the impedance measurements can be performed similarly. Besides potentiostats, several instruments based on small signal AC admittance measurements like impedance analyzers [24], LCR meters [25], lock in amplifiers [26] and frequency response analyzers [27] have been utilized to measure the response of impedance biosensors and can operate in a wide frequency range. While many these instruments are utilized in laboratory settings, they are bulky and expensive and are not suitable for point of care applications. Therefore, there is a need to develop low cost, portable and compact impedance analyzers. An example includes an impedance analyzer developed by Chuang *et. al.* that can operate in a frequency range of 1 KHz–100 KHz as shown in Figure 3 [28]. It is based on an AD5933 integrated circuit (IC) where the response signal from the impedance is sampled by the on-board ADC and a discrete Fourier transform (DFT) and communicated to a digital microcontroller through an Inter-Integrated Circuit (I²C) interface. Self-calibration functions are implemented by four sets of switching relays and precision resistors. The device can calculate optimal gain values before measurement to avoid errors due to environmental factors such as humidity or temperature. A smart gain function allows the device to automatically switch gain resistors to find the best fit for the immunosensor chip. In this way, wide range of impedance measurements without manual control can be achieved.

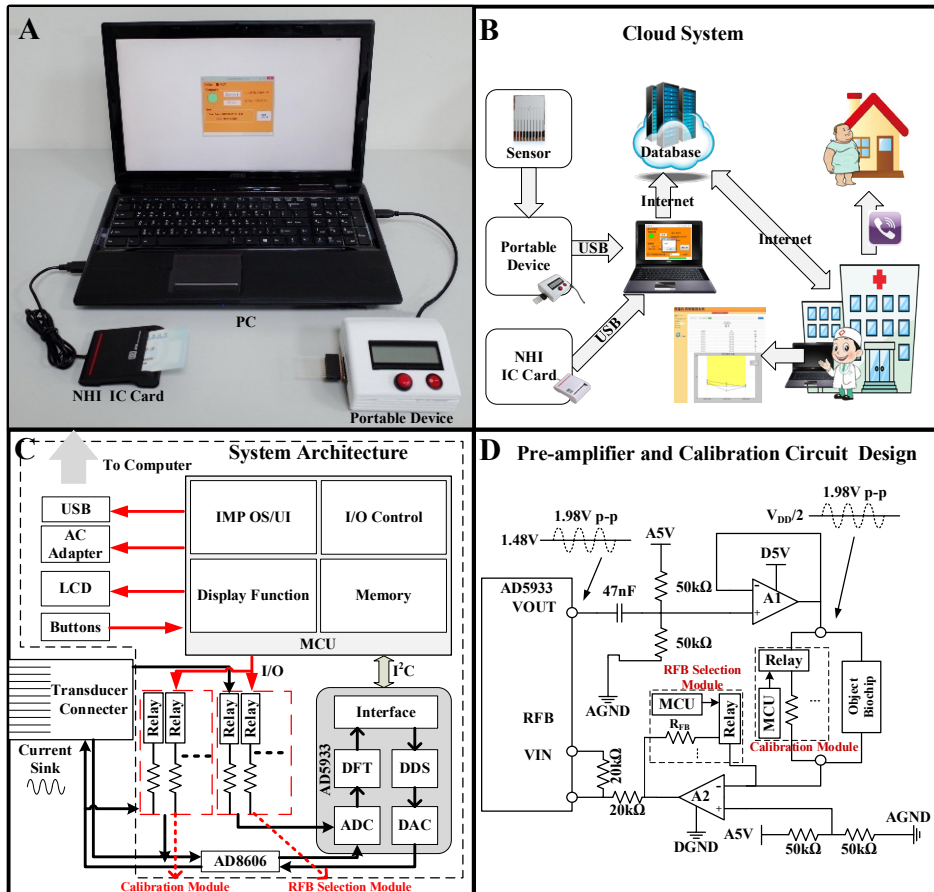


Figure 3: (a) An image of the point of care system which includes the immunosensor chip attached to the portable device for impedance measurement, a National Health Insurance (NHI) IC Card reader and personal computer. (b) A schematic of data collection and transmission to cloud data base. (c) Block diagram of portable impedance measuring device. (d) Design of pre-amplifier and calibration circuit to improve accuracy and stability by increased signal-noise ratio (SNR) during impedance analysis.

A comparison of the impedance measurements of the portable impedance device with an LCR meter at an operating frequency of 10 KHz show a maximum deviation of 3.47 %. The results obtained using the portable device can be read on the liquid crystal display (LCD) with two buttons to interface with the user. All the data including the date, patient's information and measured results from portable analyzer can then be uploaded to the patients file on the cloud database using a National Health Insurance (NHI) IC Card, USB connection and a personal computer. The doctor can then view the uploaded results and can directly contact the patient if further examination is required.

In this way, a complete system can be obtained for effective and real time diagnosis at the point of care.

8.7. DATA ANALYSIS USING EQUIVALENT CIRCUIT MODELS

Owing to the complexity of real electrochemical systems, the obtained impedance spectrum is often analyzed using simplified equivalent circuits. This circuit commonly comprises of resistances and capacitances that represent the independent physiochemical processes contributing to the overall system behavior [29]. Once this circuit is defined, the obtained experimental data is fitted to it using non-linear square fitting techniques [30]. Although simple, this technique can be risky as the same data could be fitted to several different circuit models. Therefore, it is not advisable to try to fit the obtained data to a random combination of circuit elements until a best fit is obtained. Even the best models for interfacial phenomena do not often fit at extreme frequencies or either require so many fitting parameters so as to be useless. It is more reasonable to fit the obtained data to a predefined model and changes in the circuit elements (resistance or capacitance) can then be reported as the biosensor output. This can simplify measurements so that the impedance response of the biosensor can be determined at one particular frequency or in a small frequency range where the relative change is the largest. The four basic elements used to describe impedance behavior, namely ohmic resistance, capacitance, constant phase element and Warburg impedance and their definitions are summarized in Table 1.

Table 1: Definitions, frequency dependences and phase shifts of the impedance elements used to describe biosensor systems [6].

Impedance Element	Definition	Phase Angle	Frequency Dependence
R	$Z = R$	0°	No
C	$Z = \frac{1}{j\omega C}$	90°	Yes
CPE	$Z = \frac{1}{Aj\omega^\alpha}$	0-90°	Yes
W(semi-finite)	$Z = \frac{\sigma}{\sqrt{\omega}}(1 - j)$ $\sigma = \frac{RT}{n^2 F^2 \sqrt{2}} \left(\frac{1}{\sqrt{D_o c_o}} + \frac{1}{\sqrt{D_R c_R}} \right)$	45°	Yes

ω angular frequency

D diffusion coefficient

A has the numerical value of the admittance (1/|Z|) at $\omega = 1 \text{ rad/s}$

σ Warburg coefficient

c_o, c_R concentration of oxidized and reduced species

The simplest and in fact the most commonly used electronic equivalent circuit to analyze impedance biosensors is the Randles and Ershler model [31-33] as shown in Figure 4a. It consists of the uncompensated ohmic resistance of the electrolyte solution, R_s , the double layer capacitance owing to the charging of the electrode/solution interface (C_{dl}), charge transfer resistance at the electrode/solution interface (R_{ct}) in the presence of a redox probe and the Warburg impedance (W) resulting from diffusion of ions from bulk electrolyte to the electrode surface. The circuit elements R_{ct} and W are connected in parallel to C_{dl} since the total current flowing through the working electrode is the sum of distinct contributions originating from the Faradaic process and the interfacial charging. Due to surface roughness of the electrode, the electronic properties of the interface cannot be simply described by a purely capacitive element and a constant phase element (CPE) is often used to replace C_{dl} . Since all the current must flow through the uncompensated resistance of the electrolyte solution, R_s , it is inserted as a series element. The two circuit elements, R_s and W represent the bulk properties of the electrolyte solution and the diffusion of redox probes in the solution and are thus unaffected by the presence of biomolecules on the electrode surface. On the other hand, R_{ct} and C_{dl} depend on the insulating and dielectric features of the biomolecules and are the main parameters used to analyze the response of an impedance biosensor.

A typical shape of the impedance spectrum for this circuit model is presented as a Nyquist plot (Figure 4b-i) and includes a semicircle region lying on the Z_{re} axis followed by a straight line. The straight line is observed at low frequencies and corresponds to the mass transfer limited process due to delay in diffusion

of ions from the electrolyte to the electrode surface. The semicircle observed at higher frequencies implies a charge transfer limited process. Furthermore, the shape of the spectra varies depending on the rate of charge transfer at the electrode/electrolyte interface. For a very fast electron transfer (Figure 4b-ii), only the linear part could be observed while for a very slow electron transfer (Figure 4b-iii), a large semi-circle is observed without any straight line. The interfacial phenomena and diffusional characteristics can be easily extracted from the spectra. The C_{dl} can be calculated from the frequency at the maximum of the semicircle ($\omega = 2\pi f = 1/R_{ct}C_{dl}$). The R_{ct} is represented by the semicircle diameter and the intercept of the semicircle with the Z_{re} axis at high frequencies corresponds to R_s . The 45° line can be extrapolated to the Z_{re} axis and the intercept which is equal to $R_s + R_{ct} - 2\sigma C_{dl}$ can be used to calculate the Warburg coefficient (σ) and subsequent diffusion coefficients as defined in Table 1. To simplify data analysis, the Warburg impedance could be neglected by choosing a frequency range where no straight line is observed in the Nyquist plot and the impedance response is dominated by the interfacial changes. Furthermore, it is important to choose a frequency range where a meaningful impedance spectrum can be obtained. This range is generally 0.01 Hz–1 MHz and the circuit elements that dominate at different frequencies is shown in the Bode plot in Figure 4c. At extremely low frequencies (below 1 mHz), the impedance is generally dominated by the DC conductivity of the electrolyte while inductance contributions of the electrochemical setup and connecting wires begin to influence at very high frequencies (above 1 MHz). A more detailed analysis of the circuit elements will be provided later when discussing the model of an impedance immunosensor.

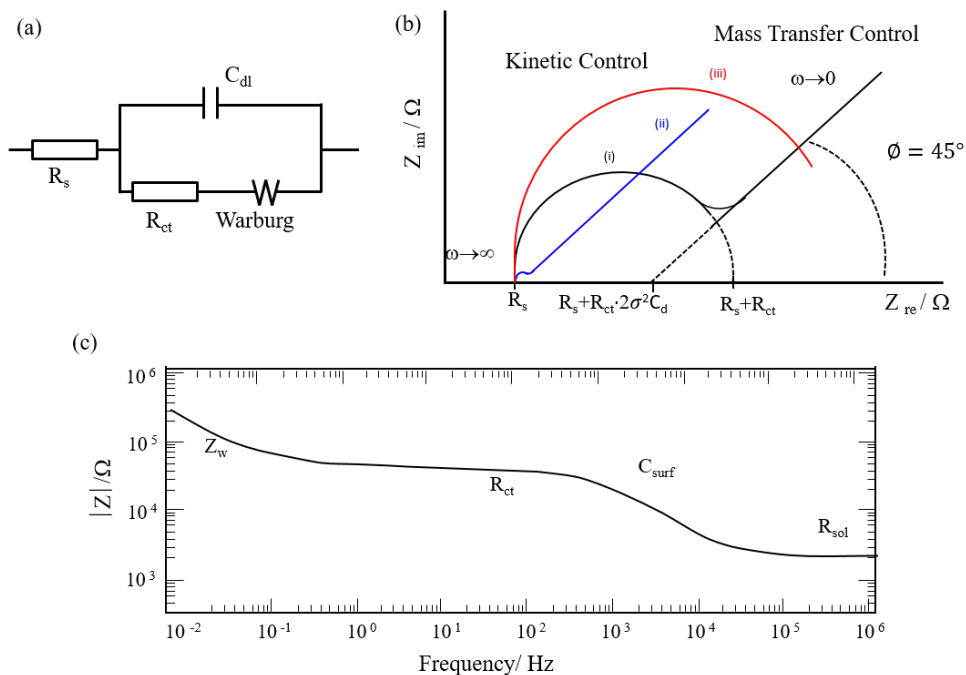


Figure 4. (a) The most commonly used equivalent circuit model to analyze impedance data, namely the Randles and Ershler model. (b) Impedance spectrums in the form of a Nyquist plots for this circuit depending on the rate of charge transfer at the electrode/electrolyte interface. (c) The circuit elements that dominate at different frequencies.

8.8. IMMOBILIZATION STRATEGIES

The development of impedance based affinity biosensors requires the immobilization of the bioreceptor on the electrode surface so that it can selectively capture the analyte of interest, thus resulting in an impedance change. To achieve sensitive and reproducible results, it is crucial that the receptor retains its original properties after immobilization. The efficacy of receptor integration with the electrode surface, availability of target binding sites, orientation and surface density all affect the final performance of affinity biosensors. Several immobilization strategies have been utilized and we will discuss a few that are applicable to impedance biosensors. While “physical” methods like adsorption and entrapment can result in high surface densities on ionic and hydrophobic surfaces, the receptor modified electrode surface often exhibits low binding efficacy and instability. Proteins, including antibodies, are known to suffer from activity losses when immobilized using physical methods which may be due to denaturation, poor orientation of

binding sites and steric hindrance as a result of overcrowding and aggregate formation [34,35]. This approach also poses challenges when the bioreceptor needs to be immobilized specifically on the electrode surface. One way of improving physical immobilization on electrode surfaces is by using AC electrokinetic techniques like dielectrophoresis (DEP) to trap the bioreceptor on the electrode surface and some examples are illustrated in Figure 5 [28,36-38]. DEP can be defined as the translational motion of a dielectric particle or biological cell in a suspended medium under the influence of a non-uniform AC electric field which acts on the particle driving it towards/against the direction of the electric field maxima.

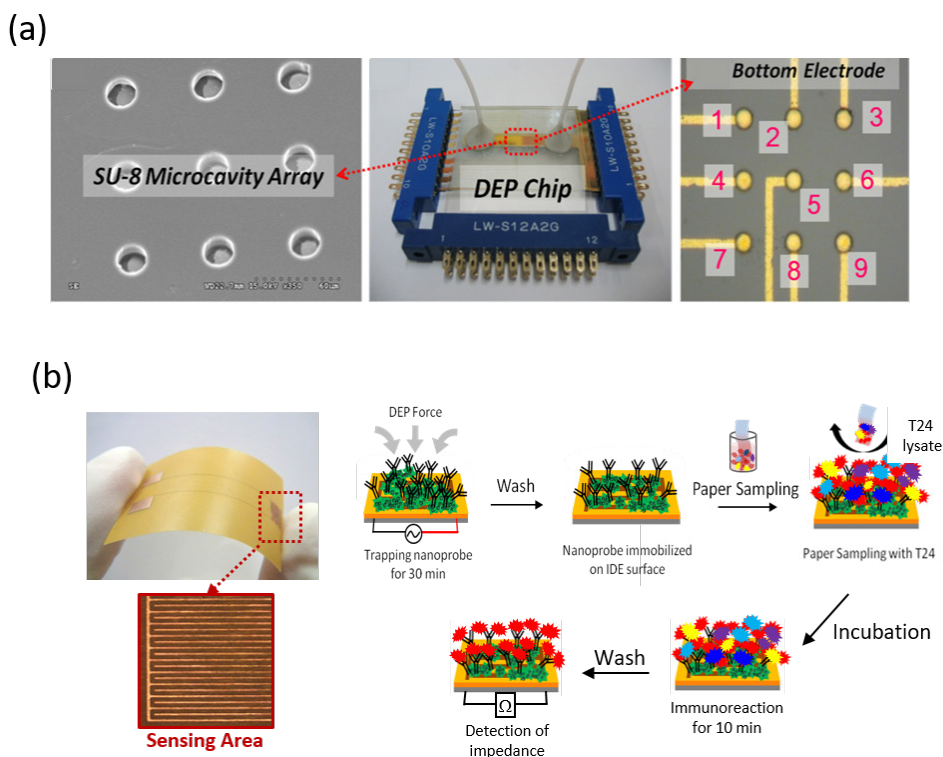


Figure 5: Manipulation of bioreceptors using dielectrophoresis for impedance biosensing. (a) Programmable trapping and release of cells in microcavities [37]. (b) Trapping of nanoprobes (antibody conjugated nanoparticles) on IDEs [38].

For impedance biosensors, controllable and stable immobilization of bioreceptor is most commonly achieved by using an intervening and chemically tailorable self-assembled monolayers (SAM). Such films can be spontaneously formed by chemisorption and self-organization from solution [39,40]. Most common types of attachment chemistries for SAM are based on

thiols bound to metallic surfaces [41] and siloxanes to oxide surfaces [42]. Thiol SAMs are the most studied and are prevalent in impedance biosensors. Generally gold electrodes have been used in impedance biosensors as they are stable and inert and enable the formation of SAM *via* thiol-gold chemistry in an ordered and reproducible way. The bioreceptor immobilization using an SAM generally requires two steps. The first one involves the formation of an SAM that consists of a molecular chain with a thiol head group and a functional terminal group (carboxylic acid, amine *etc.*). The second step involves the reaction of the recognition element with the functional group of the SAM usually through covalent linking (amide bond, carbodiimide chemistry) or by the aid of bridging molecules like glutaraldehyde. SAM films may be single component or mixed. A mixed SAM is obtained from a solution comprising two different thiols with different end-groups and chain lengths. One of the end groups is used to covalently tether the receptor while another, usually of reduced chain length, is used to minimize lateral steric hindrance to target recruitment [43,44]. Thus, SAMs with appropriate functional groups that selectively capture specific analytes are easy to immobilize and have complete blocking capabilities and stabilities. Since stable and reproducible coatings based on SAMs can be achieved only on perfectly clean and low roughness surfaces, gold electrodes are often chemically treated to remove organic moieties before SAM formation. Alternative approaches to SAM for the formation of well-ordered recognition layers include transfer of lipid bilayer or Langmuir-Blodgett films on the electrode surface [45,46]. Other protocols that have been utilized include fabrication of thin polymer films and bio affinity layers like avidin films that have high affinity for biotinylated receptors [47]. Irrespective of the chosen strategy, the biorecognition element should be immobilized in a stable way such that it retains its accessibility to the target molecule and its recognition capability. Furthermore, the electrode surface modification should be biocompatible and inert so that it does not affect the integrity of the target analyte while also providing a constant baseline signal.

8.9. MODEL OF AN IMPEDANCE IMMUNOSENSOR

To demonstrate the use of impedance based affinity biosensing, we use the model of an immunosensor which relies on the specific binding of an antibody to its corresponding antigen, resulting in the formation of a stable complex on the electrode surface. This affinity binding between antigen and antibody alters the properties of the electrode/electrolyte solution interface and can be analyzed using EIS. First, let us consider for example a bare gold electrode that is immersed in an electrolyte solution. The charged electrode surface will attract ions of opposite charge from the solution and this will cause the interface to be electrically analogous to a capacitor. This is termed as the ionic double layer capacitance (C_{dl}) and this charge accumulation prevents the electric field arising from electrode surface to penetrate far into the solution.

The characteristic length of the spatial decay of electric field is termed the Debye length and represents the range in which the applied potential can alter the charge distribution in the solution [48]. It is in this range that the attachment of the antibody to its corresponding antigen can affect the total interfacial capacitance. The value of the C_{dl} depends on many variables which include electrode potential, temperature, ionic concentration, types of ions, electrode roughness and impurity adsorption. The gold electrode surface and the ions in solution can be considered as parallel conducting plates separated by a dielectric layer and the C_{dl} be expressed as:

$$C_{dl} = \varepsilon\varepsilon_0 A/d$$

where ε is the dielectric constant of this layer, ε_0 is the permittivity of free space ($8.85419 \text{ pF m}^{-1}$), A is the surface area of the plates and d is the distance between the plates.

Next, the gold electrode surface must be functionalized with the biorecognition element which is the antibody in this case. To fabricate an efficient immunosensor, the antibodies can be immobilized in an oriented manner such that the tail region is bound to the electrode while the antigen binding region is available for immunosensing as shown in Figure 6. The gold electrode is first cleaned (*e.g.* using a Piranha solution followed by electrochemical cleaning) and immersed in a 0.1–0.5 M solution of heterobifunctional ligand (*e.g.* Cysteamine) for a certain period of time. The Cysteamine will form a self-assembled monolayer layer (SAM) on the gold electrode *via* its thiol head group while its terminal amino group can be used to covalently link the antibody. The antibody can be oxidized in a solution of sodium metaperiodate and sodium acetate. This results in the oxidation of the hydroxyl groups ($-\text{OH}$) of its carbohydrate moieties to aldehyde groups ($-\text{CHO}$) which can then react with the amino group of the Cysteamine SAM *via* peptide or amide bond formation. The immunosensor with immobilized antibody is now ready for use and can form an antigen-antibody complex during immunosensing. The impedance response after each surface modification can be measured in an electrolyte solution.

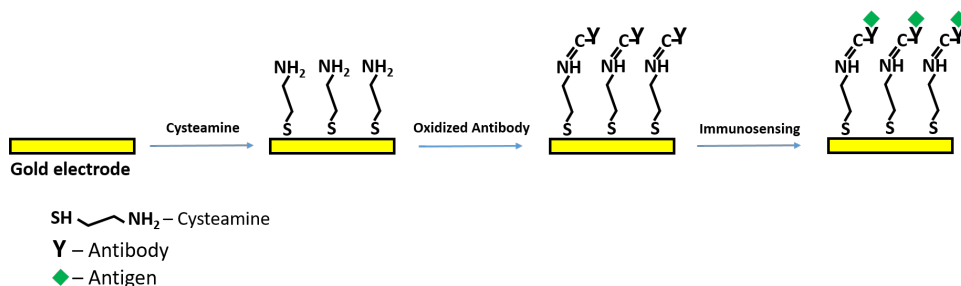


Figure 6. Fabrication of immunosensor utilizing self-assembled monolayers

When the gold electrode is modified with SAM followed by antibody and its corresponding antigen, the structure of the electrode/electrolyte interface is modified and new capacitive terms may have to be considered in series with the C_{dl} . Because of this, it makes more sense in biosensors to use the term interfacial capacitance, C_{int} , rather than C_{dl} . A decrease of the C_{int} is expected due to an increase of the distance between the plates upon the binding of the antigen to the immobilized antibody. The total interfacial capacitance arises from a combined effect of the C_{dl} and the surface modification layer (C_{mod}) due to SAM formation, antibody immobilization and subsequent antigen detection and can be expressed as:

$$\frac{1}{C_{int}} = \frac{1}{C_{dl}} + \frac{1}{C_{mod}}$$

In reality, the electrode/electrolyte interface rarely exhibits purely capacitive behavior and the phase angle deviates from $\pi/2$. The actual behavior can therefore be modeled as a constant phase element (CPE) that can be expressed mathematically as:

$$CPE = A^{-1}(j\omega)^{-n}$$

While microscopic roughness of electrode surfaces contributes to this effect [49], chemical inhomogeneities and ion absorption have also been shown to play a major role [50-52] and the extent of deviation from ideal capacitive behavior is governed by the parameter n ($n \leq 1$). Thus modelling the interfacial capacitance as a pure capacitor is too simplistic and using CPE can improve fitting of the experimental data. Generally, for biosensor applications the C_{int} may be substituted by a CPE with a value of n between 0.8 and 1 and the coefficient A becomes equal to C_{int} when n is equal to 1 [32].

Ideally, the surface modification layer (before antigen detection) should be thin and/or have a high dielectric constant so that the capacitance change due to antigen-antibody complex formation dominates the total C_{int} . Assuming that the SAM layer completely covers the electrode surface (no pinholes) and no charge transfer occurs in the absence of a redox probe, the impedance response of the immunosensor can be attributed purely to changes in the interfacial capacitance and the immunosensor can be termed as being “non-Faradaic” or “capacitive” in nature. These capacitive changes can be due to several factors like variations in dielectric properties, charge distribution due to displacement of ions or water from the electrode surface or even due to changes in protein conformation originating from the formation of the antigen-antibody complex. The resultant equivalent circuit model for a purely capacitive immunosensor consists of the interfacial capacitance in series with

the solution resistance (Figure 7a). The impedance response, as observed in the Nyquist plot appears as straight line parallel to the imaginary impedance axis while the intercept of the line with Z_{re} gives an estimate of the solution resistance (Figure 7b).

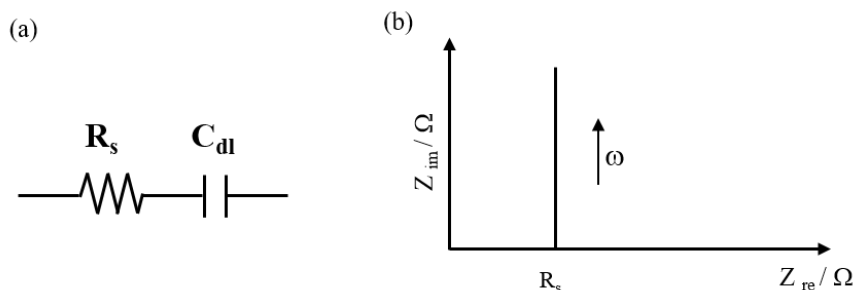


Figure 7. (a) Equivalent circuit model for a purely capacitive immunosensor and (b) the impedance response in the form of a Nyquist plot.

However, in reality there are defects in the construction of the insulating layer (presence of pin holes in the SAM) and the existence of ions and water molecules within the protein structure results in non-ideal dielectric behavior [53]. This results in charge leakage from the electrode surface into the solution. The resistance to this charge leakage, R_{leak} , can be modelled in parallel to the interfacial capacitance (Figure 8a). This effect may reduce the dynamic range and sensitivity of the capacitive immunosensor. The impedance response observed in the Nyquist plot now represents a semicircle where the low frequency intercept corresponds to R_{leak} which represents the resistance of the surface modification layers to electroactive species moving through the collapsed sites and pinholes within the film structure and reflects the protective properties of these layers (Figure 8b).

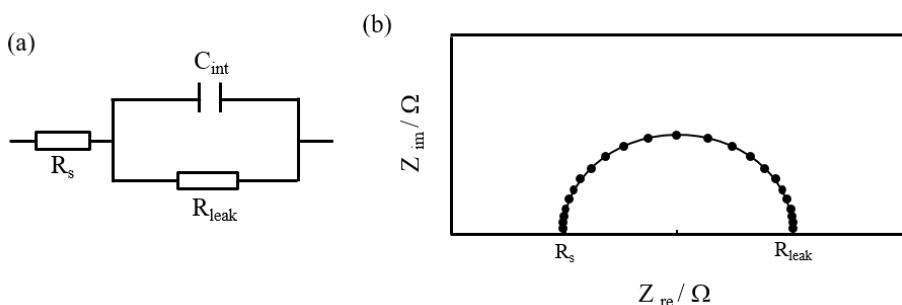


Figure 8. (a) Equivalent circuit model for a capacitive immunosensor where charge is leaking to the solution through the defects in the insulating layer and (b) the impedance response in the form a Nyquist plot.

Also as seen from the bode plots, the R_{leak} dominates at low frequencies and the phase angle is close to zero. As the frequency increases, the impedance due to the C_{int} become lower than that of R_{leak} until it dominates at which point the capacitive effects begin to dominate and the phase angle approaches 90. At significantly higher frequencies, the R_{sol} dominates the impedance response and the phase angle again approaches zero. Therefore, appropriate choice of a measurement frequency will approximate the impedance as a capacitor. This is the frequency range we prefer to make measurement in because addition of the antigen will change the interfacial capacitance. Ignoring the apparent effect of the resistances in the model will simplify the readout and post-readout processing of the electrical signals. From the magnitude and phase shown in Figure 9, this range is determined to be between 1–30 KHz for many impedance biosensors. Changes in R_{leak} can also be employed as a sensor output and can be independently assessed using cyclic voltammetry in the presence of a redox probe.

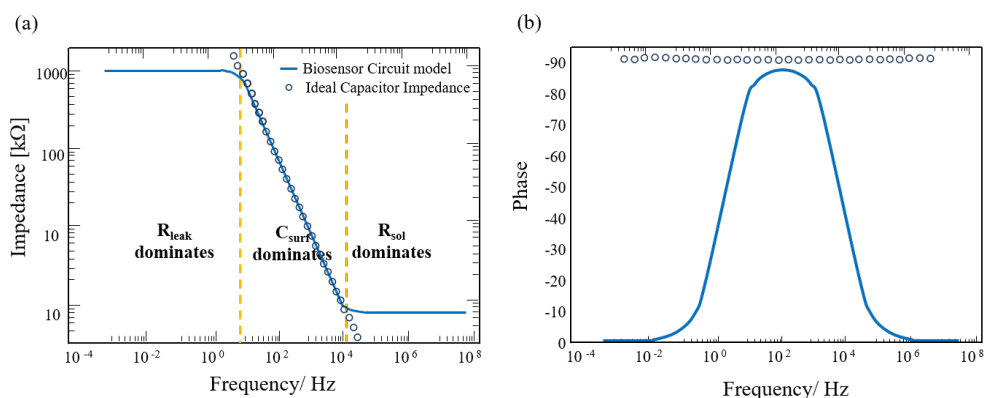


Figure 9: (a) Magnitude plot and (b) phase plot of a typical capacitive immunosensor

Now, let us consider a situation when the gold electrode surface is either partially covered by an insulating SAM layer or is coated with a conducting layer (*e.g.* conducting polymers like polypyrrole). If there are redox probes present in the measuring solution and the applied potential is such that these electroactive moieties exchange electrons across the interface, a whole new set of phenomena, known as Faradaic, appear. Redox probes like ferro/ferricyanide $[\text{Fe}(\text{CN})_6^{3-/-4-}]$ [54], ferrocene [55] and ruthenium hexaammine $[\text{Ru}(\text{NH}_3)_6^{3+/2+}]$ [56] are commonly used to monitor the ability of the modified electrode to transfer electrons. As the electrode surface is progressively modified sequentially, the interfacial charge transfer to a redox probe present in the solution becomes increasingly difficult due to the blocking effect of the SAM, antibodies, and antigens. This is described as a resistance to

charge transfer, R_{ct} , in the equivalent circuit model and is present in parallel to the C_{int} (Figure 4a). R_{ct} represents the real component of the impedance response at low frequencies (typically 0.1–10 Hz) and can be mathematically expressed in as a series combination of R_{Au} and R_{mod} which represent the constant electron transfer resistance of the unmodified gold electrode and the variable electron transfer resistance introduced by the surface modification, in the presence of the solubilized redox probe, respectively.

$$R_{ct} = R_{Au} + R_{mod}$$

When the electrode kinetics are fast, the electrochemical process is limited by mass transfer [57]. Therefore, if the applied potential is such that the electron transfer is sustained, then the supply of material to and from the bulk solution to the electrode surface is limited by the diffusion of the redox probe. In general, mass transport can be of several forms which include convection (due to stirring of solution), migration (due to charge gradient) or diffusion (due to concentration gradient). For impedimetric biosensors, experimental conditions are utilized such that the current is diffusion limited. The thickness of the interfacial diffusion layer depends on the diffusion coefficient of the redox probe, stirring rate and the temperature. Due to this mass transport limitation, an additional term is introduced into the equivalent circuit, namely the Warburg impedance, W , which appears in series with the R_{ct} .

8.10. RECENT DEVELOPMENTS IN IMPEDANCE IMMUNOSENSORS

Impedance based affinity biosensors enabling label free and direct detection are gaining widespread interest due to their suitability for point of care applications and have been demonstrated for various bioanalytes which include proteins, nucleic acids, whole cells, microorganisms, antibodies and antigens among others. In this section, we will focus on the use of impedance for immunosensing applications. In immunosensing, two strategies can be utilized which include either detection of an antigen by its specific antibody or *vice versa*. In either case, the binding event leads to a change in the electrode surface properties, although larger changes can be observed for detecting antibodies because of their higher molecular weight and low dielectric constant.

8.10.1. Non-Faradaic impedance immunosensors

Non-Faradaic or Capacitive immunosensors were initially utilized for detection of immunoreactions [58,59]. The development of the first capacitive affinity biosensor is largely credited to Newman back in 1986 who utilized interdigitated electrodes covered with a non-conducting polymer layer and an antibody probe [60]. Gebbert *et. al.* used electrochemically grown tantalum oxide with controlled thickness as an insulating layer and were able to detect anti-mouse IgG with the limit of detection (LOD) of about 1 ng ml^{-1} using mouse IgG as the probe by measuring capacitance changes at 1 KHz, although non-specific binding was quite significant [61]. Maupas *et. al.* utilized modified platinum electrodes with different polymeric layers and used a flow injection system to achieve real time immune detection of alpha fetoprotein with a relatively poorer LOD of 100 ng ml^{-1} [62]. However, they could reduce the effect of nonspecific binding using a differential mode of measurement and claimed reproducible impedance changes on an order of 1 %. Mirksky *et. al.* developed an immunosensor using anti-HSA antibodies attached to a tightly packed SAM and collected data at a frequency of 20 Hz where the impedance change was purely capacitive [63]. They used capacitive change to identify the concentration of the immobilized antibody probe and could normalize the subsequent change upon antigen binding, thus improving response reproducibility. Capacitive changes can also be used for continuous binding analysis as has been used for monitoring Human Serum Albumin (HSA) under conditions of fluid flow, thus enabling a mathematical description of the binding behavior to be identified [64]. Similarly, a highly sensitive non-Faradaic immunosensor has also been developed for the direct detection of protein interferon-g at attomolar levels (0.02 fg mL^{-1}) on polycrystalline gold electrodes that are modified with antibody attached to SAMs of cysteine or acetyl cysteine [65]. They made use of a flow cell into which controlled amount of antigen was introduced and this was followed by buffer washes. Although significant amount of nonspecific binding could be detected, they observed that this could be corrected by the subsequent washing steps. Ramakrishna *et. al.* developed a capacitive immunosensor for the detection of cardiovascular biomarkers, C-reactive protein (CRP) and myeloperoxidase, by using a gold electrode that is covered with a nanoporous silica film [66]. The exposed gold electrode at the bottom of the nanowells created by the porous silica were functionalized with dithiobis(succinimidyl propionate) to attach streptavidin followed by immobilization of biotinylated antibodies. The impedance change after antigen detection was proposed due to a perturbation of the electric double layer in each nanowell, thus resulting in a LOD in the pg ml^{-1} range. Screen printed electrodes have also been utilized for developing capacitive immunosensors. Bhalla *et. al.* developed such for the detection of cardiac biomarker, cardiac troponin I (cTnI) by attaching anti-cTnI antibodies to citrate capped gold nanoparticles deposited onto screen printed electrodes [67]. Besides the use of single planar electrodes, capacitive immunosensors

have commonly been fabricated using interdigitated electrodes (IDEs). Dutra *et al.* reported an immunosensor for cardiac biomarker, for cardiac troponin T (cTnT) based on capacitive changes after antigen binding on two planar aluminum electrodes separated by a distance of 2 mm with a detection limit down to sub ng ml^{-1} levels [68]. Recently, Chuang *et al.* developed an impedance immunosensor utilizing an interdigitated microelectrode array for the detection of bladder cancer biomarker, Galectin-1 (Gal-1) [28]. To improve sensitivity and immobilization efficiency, they have utilized nanoprobe (Gal-1 antibodies conjugated to alumina nanoparticles through silane modification) that are trapped on the microelectrode surface using programmable dielectrophoretic manipulations. The impedance response due to capacitive changes are calculated at 10 KHz where the maximum change is observed. The immunosensor shows good specificity for Gal-1 detection and an observed LOD in the pg ml^{-1} range in buffer and human urine spiked samples.

8.10.2. Faradaic impedance immunosensors

Faradaic impedance immunosensors have also been developed and normally utilize the change in resistance to charge transfer, R_{ct} , to monitor immunoreactions. An example is the detection of human mammary tumor associated glycoprotein which resulted in a change in R_{ct} after being captured by specific antibodies that were immobilized on gold electrode *via* spontaneous absorption [69]. The majority of Faradaic immunosensors utilize detector antibodies that are anchored on the electrode surface and are able to detect various targets in aqueous solution with achievable limits of detection in the sub ng ml^{-1} range. An immunoassay was developed for the detection of murine double mutant 2, a brain cancer biomarker, based on an antibody immobilized on cysteamine SAM modified polycrystalline gold electrode [70]. An LOD in sub pg ml^{-1} range was achieved in buffer solutions and the sensitivity was almost replicated in very dilute homogenous brain tissue samples. Similarly, a Faradaic immunosensor was also developed for the detection of serum cytokine, Interleukin-12, which is a biomarker for multiple sclerosis by immobilizing monoclonal antibodies on screen printed gold electrodes [71]. While they observed detection limits in the pg ml^{-1} range in buffer solutions, the assay was significantly less sensitive in serum. In order to improve assay sensitivity, Zhu *et al.* fabricated a faradic EIS immunosensor for CRP detection that utilized a three dimensional ordered macroporous gold film that was electrochemically deposited using a template consisting of silica spheres [72]. This macroporous gold electrode film resulted in a 14-fold increase in the surface area as compared to conventional planar electrodes. This should result in a significant increase in the number of antibodies immobilized *via* SAM and consequently reduced detection limits down to 0.1 ng ml^{-1} in buffer solutions. In a similar manner, an assay for carcinoembryonic antigen (CEA) was developed in which antibodies were first

coupled to nanoparticles and the bioconjugates were then trapped on a gold electrode that was modified with a non-conducting polymer film obtained by electro-copolymerization with o-aminophenol (OAP) [73]. The formation of the antibody-antigen complex resulted in an increase in R_{ct} in the presence of a $\text{Fe}(\text{CN})_6^{3-/4-}$ redox probe with detection limit range of 0.5–20 ng ml⁻¹. Faradaic immunosensors have generally been considered more sensitive as compared to capacitive measurements made at electrically blocked electrodes. However, the use of the ferro/ferricyanide redox probe system has been found to have detrimental effects on SAMs and reduce the activity of the immobilized proteins [74]. Furthermore, the observed signal change for affinity binding might not always be large as the small inorganic redox probes can easily penetrate through pinholes present in the SAM and the biorecognition layer. To improve sensitivity of Faradaic immunosensors, bulky redox molecules like NADH or redox enzymes like glucose oxidase have also been proposed instead on small redox species [75]. Enhancement in sensitivities can also be achieved by applying special approaches to immobilize the recognition element using conductive polymers like polypyrrol. This can result in an improved immunosensor response as the conductivity of the polymer film is strongly affected by conformational changes induced during the binding event [76,77]. Biotinylated polypyrrol films have been used to immobilize biotinylated antibodies *via* avidin [78]. The antigen binding results in an increase in the R_{ct} with a LOD of 10 pg ml⁻¹ observed for human IgG. In a similar direction, immunoassays have been reported where a change in ion conductivity of lipid bilayers with incorporated ion channels has been utilized for antibody-antigen detection.

8.10.3. Amplification strategies

Despite the potential for direct binding analysis, many impedance immunosensors suffer from the disadvantage that the observed interfacial changes (changes in C_{int} and/or R_{ct}) are relatively small. This has led to the use of novel strategies that have been utilized to amplify the impedance response. One smart amplification approach taken from conventional immunoassays like ELISA is the use of a secondary antibody bound to an enzyme label that results in a sandwich like structure on the electrode surface. Bressler *et al.* developed a capacitive immunosensor based on passivated IDEs and combined the original antibody-antigen interaction with a second binding event that attached a secondary antibody labeled with the enzyme catalase to the electrode surface. The catalase converts hydrogen peroxide to oxygen and the bubbles formed at the electrode surface drastically alter the dielectric properties, thus allowing very sensitive detection [79]. An enzyme label can also catalyze the formation of insoluble products that can precipitate on the electrode surface, thus amplifying changes in R_{ct} and C_{dl} [80,81]. One of the most commonly used enzyme labels for amplifying immunoreaction response

is horseradish peroxidase (HRP) and screen printed electrodes have found to be suitable transducer for this kind of amplification [82]. Besides enzymes, nanoparticles have also been used for signal amplification. Firstly, nanoparticles have been used to modify the surface of electrodes before immobilization of recognition elements. This provides advantages like enhanced surface areas and increased concentration of recognition elements, thus resulting in amplified signals [83]. Examples include electrode modification with carbon nanotubes [84] or gold nanoparticles [85]. Secondly, nanoparticles have also been used as labels similar to enzymes to form a sandwich assay which will further alter the interfacial properties and the conversion of the redox probe will change at the electrode surface. An example includes the use of gold nanoparticle labeled antibodies to amplify the electron transfer resistance arising from the binding of the antigen to the immunosensor surface [86]. An interesting amplification strategy was proposed when using IDEs for DNA detection, and is also suitable for immunosensing. It includes the use of gold nanoparticle labeling followed by an additional step where the catalytic properties of gold are used to deposit silver, thus resulting in enlargement of nanoparticles [87,88]. When this enlargement proceeds to an extent where the surface particles contact each other, a conductive pathway is developed across the two interdigitated electrodes, thus resulting in ultrasensitive detection. While improved sensitivities can be achieved, some of these amplification techniques utilizing additional labels often require multiple steps, equipped laboratories and trained professionals and may not be suitable for point of care analysis.

8.11. CONCLUSION

The potential of impedance as a transduction mechanism for biorecognition events has been illustrated by the various examples in literature. Interdigitated electrodes and amplification strategies have been shown to significantly improve the impedance response. However, further research is still required to improve reproducibility and sensitivity of analyte detection, especially in real samples which are far more complex than spiked buffer samples. Furthermore, the presence of interfering species often results in non-specific binding which increases the reported limit of detection, and this is one of the major issues associated with impedance and in particular capacitive biosensing. While a complete impedance spectrum over a wide frequency range has often been utilized for characterization of electrode surfaces, it is often time consuming and not necessarily needed. The ability to directly detect affinity binding by using a frequency at which either the change in interfacial capacitance or charge transfer resistance is maximum is a very attractive option for biosensing applications. While still needing further improvements, impedance based biosensors can enable low limits of detection without the need for

additional labeling, making them highly suitable for point of care diagnostic applications.

REFERENCES

1. D.R. Thévenot, K. Toth, R.A. Durst, G.S. Wilson. *Biosens. Bioelectron.* **16** (2001) 121-131.
2. T.G. Drummond, M.G. Hill, J.K. Barton. *Nat. Biotechnol.* **21** (2003) 1192.
3. S.J. Park, T.A. Taton, C. A. Mirkin. *Science.* **295** (2002) 1503-1506.
4. G. Zheng, F. Patolsky, Y. Cui, W.U. Wang, C.M. Lieber. *Nat. Biotechnol.* **23** (2005) 1294-1301.
5. D. Grieshaber, R. MacKenzie, J. Voros, E. Reimhult. *Sensors.* **8** (2008) 1400-1458.
6. F. Lisdat, D. Schafer. *Anal. Bioanal. Chem.* **391** (2008) 1555-1567.
7. R. Singh, I.I. Suni. *J. Electrochem. Soc.* **157** (2010) J334-J337.
8. Y. Li, R. Afrasiabi, F. Fathi, N. Wang, C. Xiang, R. Love, et al. *Biosens. Bioelectron.* **58** (2014) 193-199.
9. L. Das, S. Das, J. Chatterjee. *J. Med. Eng.* **5** (2015) 636075.
10. R. Elshafey, A.C. Tavares, M. Siaj, M. Zourob. *Biosens. Bioelectron.* **50** (2013) 143-149.
11. H. Ma, R.W.R. Wallbank, R. Chaji, J. Li, Y. Suzuki, C. Jiggins. *Sci. Rep.* **3** (2013).
12. J. Wang. *Analytical Electrochemistry*, John Wiley & Sons, New Jersey, USA, 2006.
13. B.R. Eggins. *Chemical Sensors and Biosensors*, John Wiley & Sons, West Sussex., England, 2002.
14. *Bioelectrochemistry Fundamentals, Experimental Techniques and Applications*, ed. P. N. Bartlett, John Wiley & Sons, West Sussex., England, 2008.
15. A.B. Kharitonov, L. Alfonta, E. Katz, I. Willner. *Electroanal. J. Chem.* **487** (2000) 133.
16. G. Barbero, A.L. Alexe-Ionescu, I. Lelidis. *J. Appl. Physics* **98** (2005) 113703.
17. P. Vanysek. *Can. J. Chem.* **75** (1997) 1635-1642.
18. N.J. Ronkainen-Matsuno, J.H. Thomas., H.B. Halsall, W.R. Heineman. *Trends Anal. Chem.* **21**(4) (2002) 213.
19. O. Niwa, M. Morita, H. Tabei. *Anal. Chem.* **62** (1990) 447.
20. C. Amatore, B. Fosset. *J. Electroanal. Chem.* **256** (1988) 255.
21. Ciszowska M., Stojek Z., *Electroanal. Chem.* **466** (1999) 129.
22. L. Montelius, J.O. Tegenfeldt, T.G.I. Ling. *J. Vac. Sci. Technol. A* **13** (1995) 1755-1758.
23. P. Van Gerwen, W. Laureyn, W. Laureys, G. Huyberechts, M. De Beeck, K. Baert, J. Suls, W. Sansen, P. Jacobs, L. Hermans, R. Mertens. *Sens Actuators B* **49** (1998) 73.
24. A. Gebbert, M. Alvarez-Icaza, W. Stocklein, R.D. Schmid. *Anal. Chem.* **64** (1992) 997.
25. H. Berney, J. Alderman, W. Lane, J.K. Collins. *Sens. Actuators.* **B44** (1997) 578.
26. E. Souteyrand, J.R. Martin, C. Martelet. *Sens. Actuators.* **B20** (1994) 63.
27. T.L. Lasseter, W. Cai, R.J. Hamers. *The Analyst.* **129** (2004) 3.
28. C. Chuang, Y. Du, T. Wu, C. Chen, D. Lee, et al. *Biosens. Bioelectronics* **84** (2016) 126-132.

29. D.D. Macdonald. *Electrochimica Acta* **51**(8-9) (2006) 1376.
30. J.R. Macdonald, J. Schoonman, A.P. Lehen. *J. Electroanal. Chem.* **131** (1982) 77.
31. R.N. Vyas, K.Y. Li, B. Wang. *Phys J. Chem. B* **114** (2010) 15818–15824.
32. Z.B. Stoynov, B.M. Grafov, B.S. Savova-Stoynova, V.V. Elkin. *Electrochemical Impedance*. Nauka, Moscow, 1991.
33. J.E.B. Randles. *Discuss Faraday Soc.* **1** (1947) 11.
34. F. Heitz, N. Van Mau. *Biochimica et Biophysica Acta* **1597** (2002) 1–11.
35. J.E. Butler. *Methods* **22** (2000) 22–23.
36. L. Yang. *Talanta* **80** (2009) 551–558.
37. C.H. Chuang, Y.W. Huang, Y.T. Wu. *Sensors* (2011) 11021–11035.
38. C.H. Chuang, Y. Yu, D.H.C. Lee, T.F. Wu, C.H. Chen, S.M. Chen, H.P. Wu, Y.W. Huang. *Microfluidics and Nanofluidics* **16**(5) (2014) 869–877.
39. R. Rickert, W. Gopel, W. Beck, G. Jung, P. Heiduschka. *Biosens. Bioelectron.* **11** (1996) 757.15.
40. C.D. Bain, E.B. Troughton, Y.T. Tao, J. Evall, G.M. Whitesides, R.G. Nuzzo. *J. Am. Chem. Soc.* **111** (1989) 321.
41. J.C. Love, L.A. Nuzzo, J.K. Kriebel, R.G. Nuzzo, G.M. Whitesides. *Chem.Rev.* **105**(4) (2005) 1103.
42. D.K. Aswal, S. Lenfant, D. Guerin, J.V. Yakhmi, D. Vuillaume. *Analytica Chimica Acta* **568**(1-2) (2006) 84.
43. N.C. Pesquero, M.M. Pedroso, A.M. Watanabe, M.H. Goldman, R.C. Faria, M.C. Roque-Barreira, P.R. Bueno. *Biosens. Bioelectron.* **26** (2010) 36–42.
44. P.R. Bueno, L.M. Gonçalves, F.C. Dos Santos, M.L. Dos Santos, A.A. Barros, R.C. Faria. *Anal. Lett.* **46** (2013) 258–265.
45. A. Barraud, H. Perrot, V. Billard, C. Martelet, J. Therasse. *Biosens. Bioelectron.* **8** (1993) 39.
46. L.G. Wang, Y.H. Li, H.T. Tien. *Bioelectrochem. Bioenerg.* **36**(2) (1995) 145.
47. R. Orth, T.G. Clark, H.G. Craighead. *Biomedical Microdev.* **5** (2003) 29–34.
48. M.M. Kohonen, M.E. Karaman, R.M. Pashley. *Langmuir* **16**(13) (2000) 5749–5753.
49. S.H. Liu. *Physical Rev. Lett.* **55**(5) (1985) 529.
50. Z. Kerner, T. Pajkossy. *Electrochimica Acta* **46**(2-3) (2000) 207.
51. J.B. Bates, Y.T. Chu, W.T. Stribling. *Physical Rev. Lett.* **60**(7) (1988) 627.
52. F. Heer, W. Franks, A. Blau, S. Taschini, C. Ziegler, A. Hierlemann, H. Baltes. *Biosensors Bioelectronics* **20**(2) (2004) 358.
53. M.I. Prodromidis. *Electrochim. Acta* **55** (2010) 4227.
54. M. Tolba, M.U. Ahmed, C. Tlili, F. Eichenseher, M.J. Loessner, M. Zourob. *Analyst* **137** (2012) 5749–5756.
55. A.E. Radi, J.L.A. Sanchez, E. Baldrich, C.K. O’Sullivan. *Chem J. Am. Soc.* **128** (2006) 117–124.
56. V. Ganesh, S.K. Pal, S. Kumar, V. Lakshminarayanan. *J. Colloid Interface Sci.* **296** (2006) 195–203.
57. D.R. Franceschetti, J.R. Macdonald. *J. Electroanal. Chem.* **101** (1979) 307–316.
58. H. Taira, K. Nakano, M. Maeda, M. Takagi. *Anal. Sci.* **9** (1993) 199.
59. P. Bataillard, F. Gardies, N. Jaffrezicrenault, C. Martelet, B. Colin, B. Mandrand. *Anal. Chem.* **60** (1988) 2374.
60. A.L. Newman, K.W. Hunter, W.D. Stanbro. *Chemical Sensors: 2nd International Meeting. Proceedings*. 1986, pp. 596–598.

61. A. Gebbert, M. Alvarezicaza, W. Stocklein, R.D. Schmid. *Anal. Chem.* **64**(9) (1992) 997.
62. H. Maupas, A.P. Soldatkin, C. Martelet, N. Jaffrezic-Renault, B. Mandrand. *J. Electroanal. Chem.* **421**(1-2) (1997) 165.
63. V.M. Mirsky, M. Riepl, O.S. Wolfbeis. *Biosens. Bioelectron.* **12**(9/10) (1997) 977.
64. M. Hedstrom, I.Y. Galaev, B. Mattiasson. *Biosens. Bioelectron.* **21** (2005) 41.
65. M. Dijkstra, B. Kamp, J.C. Hoogvliet, W.P. Bennekom. *Anal. Chem.* **73** (2001) 901–907.
66. K.C. Lin, V. Kunduru, M. Bothara, K. Rege, S. Prasad, B.L. Ramakrishna, *Biosens. Bioelectron.* **25** (2010) 336–2342.
67. V. Bhalla, S. Carrara, P. Sharma, Y. Nangia, C.R. Suri. *Sens. Actuators B* **161** (2012) 761–768.
68. E.A. de Vasconcelos, N.G. Peres, C.O. Pereira, V.L. da Silva, E.F. da Silva, R.F. Dutra. *Biosens. Bioelectron.* **25** (2009) 870–876.
69. M. Jie, C.Y. Ming, D. Jing, L.S. Cheng, L.H. Na, F. Jun, C.Y. Xiang. *Electrochem. Commun.* **1** (1999) 425.
70. R. Elshafey, C. Tlili, A. Abulrob, A.C. Tavares, M. Zourob. *Biosens. Bioelectron.* **39** (2013) 220–225.
71. K. Bhavsar, A. Fairchild, E. Alonas, D.K. Bishop, J.T. La Belle, J. Sweeney, T.L. Alford, L. Joshi. *Biosens. Bioelectron.* **25** (2009) 506–509.
72. X.J. Chen, Y.Y. Wang, J.J. Zhou, W. Yan, X.H. Li, J.J. Zhu. *Anal. Chem.* **80** (2008) 2133–2140.
73. H. Tang, J.H. Chen, L.H. Nie, Y.F. Kuang, S.Z. Yao. *Biosens. Bioelectron.* **22** (2007) 1061–1067.
74. J. Rickert, W. Gopel, W. Beck, G. Jung, P. Heiduschka. *Biosens. Bioelectron.* **11** (1996) 757.
75. B.Y. Won, H.C. Choi, K.H. Kim, S.Y. Byun, H.S. Kim, H.C. Yoon. *Biotechnol. Bioeng.* **89** (2005) 815.
76. A. Sargent, T. Loi, S. Gal, O.A. Sadik. *J. Electroanal. Chem.* **470** (1999) 144.
77. O. Ouerghi, A. Senillou, N. Jaffrezic-Renault, C. Martelet, H. Ben Ouada, S. Cosnier. *J. Electroanal. Chem.* **501** (2001) 62.
78. O. Ouerghi, A. Touhami, N. Jaffrezic-Renault, C. Martelet, H. Ben Ouada, S. Cosnier. *Bioelectrochemistry* **56** (2002) 131.
79. H.S. Bresler, M.J. Lenkevich, J.F. Murdock, A.L. Newman, Roblin RO (1992), In Biosensor design and application. American Chemical Society Mathewson PR, Finley JW (eds), American Chemical Society, Washington, DC.
80. A. Bardea, E. Katz, I. Willner. *Electroanalysis.* **12** (2000) 1097.
81. L. Alfonta, A. Bardea, O. Khersonsky, E. Katz, I. Willner. *Biosens Bioelectron.* **16** (2001) 675.
82. T. Balkenhohl, F. Lisdat. *Anal. Chim. Acta.* **597** (2007) 50.
83. S. Zhang, F. Huang, B.H. Liu, J.J. Ding, X. Xu, J.L. Kong. *Talanta* **71** (2007) 874.
84. Y. Xu, X.Y. Ye, L. Yang, P.A. He, Y.Z. Fang. *Electroanalysis* **18** (2006) 1471.
85. Y.Z. Fu, R. Yuan, L. Xu, Y.Q. Chai, X. Zhong, D.P. Tang. *Biochem. Eng. J.* **23** (2005) 37.
86. H. Chen, J.H. Jiang, Y. Huang, T. Deng, J.S. Li, G.L. Shen, R.Q. Yu. *Sens Actuators B* **117** (2006) 211.
87. R. Möller, A. Csáki, J.M. Köhler, W. Fritsche. *Langmuir* **17** (2001) 5426.
88. S.J. Park, T.A. Taton, C.A. Mirkin. *Science* **295** (2002) 1503.

